



UDC 528.481

INVESTIGATION OF THE EFFECTS OF KAHRAMANMARAŞ EARTHQUAKE SERIES ON CYPRUS ARC, DEAD SEA FAULT, HATAY REGIONS AND STATIONS CLOSE TO TWO EARTHQUAKES EPICENTERS

Atınç PIRTI  
Department of Geomatic Engineering, Yıldız Technical University, Esenler, Istanbul, Türkiye

Article History:

- received 01 August 2023
- accepted 29 August 2024

Abstract. In various parts of the globe, there have been several earthquakes of a modest size. Monitoring the change of the points over time is a key component of typical techniques for extracting dynamic responses. This technique was unable to completely extract all of the earthquake's dynamic properties. The GNSS precise point positioning (PPP) may be a useful tool for obtaining values of the point's displacement that are more exact up to millimeters, which can help to overcome these flaws and evaluate the seismic wave of such earthquakes. Ultimately, PPP is a crucial tool for getting the precise observations. In this study, Canadian Spatial Reference System Precise Point Positioning (CSRS-PPP) approach to analyze the station's displacement components and the station's heights in periods from the two Kahramanmaraş earthquakes. The earthquake sequences that occurred in Turkey's Kahramanmaraş in 2023 is an example of complicated faulting brought on by interactions between three plates close to the Hatay Triple Junction (HTJ). While the relative plate movements in this area are minimal (usually less than 10 mm/year), even sluggish plate motion zones may nevertheless see earthquakes that are quite destructive. Due to the three-plate system's unusual geometry, a number of large earthquakes with very varied fault orientations were active throughout this series. A 7.8-magnitude earthquake happened on February 6, 2023 in southern Turkey, close to Syria's northern border. A magnitude 7.5 earthquake, situated about 95 kilometers to the southwest, was occurred nine hours after the first one. The first earthquake was as big as the most powerful one ever recorded there in 1939 and was the most catastrophic to strike earthquake-prone Turkey in more than 20 years. In this study, the effects of two earthquakes in Kahramanmaraş were investigated on the Cyprus Arc, the Dead Sea fault, Hatay and the points close to two earthquakes zone. In the obtained results, it was computed that the greatest horizontal displacement occurred at the HAT2 station with 68.97 cm.

Keywords: Kahramanmaraş earthquake sequences 2023, displacements, accuracy, deformation.

✉ Corresponding author. E-mail: atinc@yildiz.edu.tr

1. Introduction

Despite the current modest seismicity, big and destructive earthquakes have previously occurred in southern Turkey and northern Syria. While the particular locations and magnitudes of these earthquakes are unknown, Aleppo, in Syria, has traditionally been ravaged by big earthquakes. An estimated M 7.1 earthquake struck Aleppo in 1138, while an estimated M 7.0 earthquake struck the city in 1822 (Ambraseys, 2009). The movement of the Hatay Triple Junction has left a complicated plate boundary fault pattern in the area of these earthquakes, including a thin segment of the African plate sandwiched between the Arabian and Anatolian plates, Figure 1a. When the series of earthquakes occurred, changes in the region's crustal stress probably caused or helped cause more fault rupture on nearby faults, including the Sürgü fault, which was the

site of the M 7.5 earthquake and significant aftershock activity. The vast zone of damage resulted from the series, which started on the Dead Sea fault's northernmost segment and included rupture along a sizeable portion of the East Anatolian fault (Aktug et al., 2016; Akyuz et al., 2006; Emre et al., 2018; Palutoğlu & Sasmaz, 2017; Tari et al., 2014).

A strike-slip system with a northward tendency that accommodates the differential motion of the African and Arabian plates is the Dead Sea fault, which is located farther south. At the southern end of the Dead Sea fault, where speed decreases farther north, the Arabian plate advances past the African plate in a northerly direction at a rate of roughly 10 mm/year, Figure 1a. In the historically highly populated Levant area, earthquake activity along the Dead Sea fault has been a substantial risk (eastern Mediterranean). In a complex deformation zone

in southern Turkey, the eastern end of the Cyprus Arc, the northern end of the Dead Sea fault, and the western end of the East Anatolian fault all merge (Duman & Emre, 2013; Akyuz et al., 2006; Elhadidy et al., 2021; Mahmoud et al., 2013). The Dead Sea fault and the East Anatolian fault met in the area where the 2023 M 7.8 and M 7.5 earthquakes struck. Both the northernmost section of the Dead Sea fault and a large piece of the southwestern third of the East Anatolian fault were ruptured by this earthquake series. Starting with the 2020 M 6.7 earthquake sequence and the recent 2023 M 7.8 and M 7.5 earthquake sequences, much of the southern section of the East Anatolian fault has ruptured. The M 7.8 earthquake that struck on February 6, 2023, was located close to Syria's northern border in southern Turkey. This earthquake was followed about 9 hours later by an M 7.5 earthquake around 95 kilometers, Figure 1b. The Dead Sea and East Anatolian fault systems intersect in the area where the M 7.8 and related aftershocks occurred. According to early information, the M 7.8 earthquake occurred close to a triple plate intersection between the Arabian, African, and Anatolian blocks. The Dead Sea fault accommodates the northward migration of the Arabian Peninsula with respect to the African plate, whereas the East Anatolian fault accommodates the westward movement of Turkey into the Aegean Sea. While seismic activity in the area of the M 7.5 earthquake series that occurred on February 6, 2023 is mild (M 7), compared to the surrounding plate boundary zones in Turkey, it is nonetheless active (U.S. Geological Survey, 2023; Hancılar et al., 2023; Reitman et al., 2023). The Sürgü fault, which is located just west of the East Anatolian fault, is where this incident's epicenter is located, Figure 1b. CORS-TR stations, which are a part of the CORS-TR network and are located close to the epicenters of two Kahramanmaraş (06.02.2023) earthquakes, were used in this study to process (using the static/kinematic method) and analyze these GNSS data. The two earthquakes' three-dimensional displacements in the study region were computed by processing the time series produced by the daily solution (kinematic-static method), (06.02.2023).

2. Materials and methods

2.1. Kinematic method

Kinematic measurements has many similarities to static surveys. With one receiver, the base, occupying a station in a known location and another, the rover, gathering information on sites of interest, a kinematic survey needs two receivers collecting observations concurrently from a pair of stations. Additionally, it employs computational techniques for relative position that are comparable to those employed in static surveys. As a result, it mandates that the integer ambiguities be solved before the survey is launched. The duration of each session is the primary distinction between static and kinematic surveying methods. The position of the

rover receiver in a kinematic survey may only be known from measurements from a single epoch. Static surveying techniques need significantly longer sessions than are generally utilized in kinematic surveys in order to establish control points. As was already said, kinematic surveys often do not have the same precision as static surveys. The absence of repeated observations and the duration of the session are some of the limiting factors. Throughout the duration of the observation, all receivers must concurrently gather signals from at least four of the same satellites. Kinematic surveying works best with dual-frequency receivers, while single-frequency receivers may be utilized as well. The technique produces positional accuracy to within a few millimeters, making it ideal for the majority of surveying, mapping, and stakeout. It is also fantastic for dynamic surveying, which is when the rover station is moving. Kinematic surveying may provide results right away when used in real-time kinematic (RTK) mode or in the office when used in post-process kinematic (PPK) mode. While the receiver is moving, kinematic surveying offers positioning. It should be emphasized that, much like with static surveys, post processed kinematic (PPK) surveys may lessen the impacts of geomagnetic storms that cause ephemeral error by employing one of the exact ephemerides that are readily accessible. Additionally, because a radio connection between the base and rover is not necessary during a PPK survey, radio blackouts are not a concern (Wolf & Ghilani, 2002; Pirtı et al., 2023; Hofmann-Wellenhof et al., 2001).

2.2. Precise Point Positioning (PPP) solution

A PPP solution relies on GNSS satellite clock and orbit adjustments, which are computed and then sent to the end users via satellite. PPP is a positioning approach that models or eliminates GNSS system errors to give a high degree of location accuracy from a single receiver. Receiving these adjustments enables decimeter-level, or better location, without the need for a base station. Up to 1–2 centimeters of precision are provided by PPP. It takes time for a typical PPP solution to converge to decimeter precision and eliminate any local biases caused by factors including the atmosphere, multipath environment, and satellite geometry. The quality of the corrections and how they are applied in the receiver determine the actual accuracy that is obtained and the required convergence time, but the main error sources for PPP that affect its accuracy are the ionospheric delay, satellite orbit and clock corrections, the tropospheric delay, and carrier-phase ambiguities. An Extended Kalman Filter (EKF) is used for the PPP estimation. Position, receiver clock error, tropospheric delay and carrier-phase ambiguities are estimated EKF states. EKF minimizes noise in the system and enables estimating position with centimeter level accuracy. The estimates for the EKF states are improved with successive GNSS measurements, until they converge to stable and accurate values. The typical con-

vergence time of PPP to under 10 cm horizontal error is between 20 and 40 minutes, but it depends on the number of satellites available, satellite geometry, quality of the correction products, receiver multipath environment and atmospheric conditions. This paper examined the use of the PPP technique to achieve high accuracy of the station network displacements in response to earthquake shaking. It is extracted the values of the movements of the points in three dimensions, X, Y, and H. It is clear that PPP represents a significant advancement in the development of high accuracy positioning (Ehiorobo & Ehigintor Irughe, 2012; Pirtı et al., 2023; CSRS-PPP Online Processing, 2023; Tu, 2014).

2.3. Study site

Three plate-boundary fault segments that converge at the Hatay Triple Junction were ruptured by the M 7.8 earthquake (HTJ), Figure 1a. The border between the African, Arabian, and Anatolian plates is defined by this triple junction. The HTJ migrates, as is characteristic of most triple junctions. Since its development about 20–15 Ma ago, the East Anatolian fault—the rate of plate motion between the Arabian and Anatolian plates—has moved along the eastern edge of the Anatolian block.

The present plate arrangement in the area of the M 7.8 earthquake is complicated as a consequence of this triple junction movement. Earthquake rupture started on the Dead Sea fault (DSF), signifying motion between the Arabian and African plates. The HTJ was reached when the fault rupture moved north. The rupture then proceeded bilaterally along the EAF. The motion between the Anatolian and Arabian plates is represented by the rupture to the northeast, while the motion between the Anatolian and African plates is represented by the rupture spreading to the southwest. Two fault segments that are connected by a thin section of the African plate ruptured in close proximity to the HTJ, Figure 1a (Elhadidy et al., 2021; Mahmoud et al., 2013; Tari et al., 2014).

Two devastating earthquakes measuring 7.8 and 7.5 on the Richter scale rocked Pazarcık and Elbistan in Kahramanmaraş, Turkey, on February 6, 2023, Figure 1b. The eleven provinces where a state of emergency has been declared have seen devastating effects. Hatay, Kahramanmaraş, and Gaziantep are supposedly hardest, as are Adyaman, Kilis, Hatay, Malatya, Diyarbakır, Adana, Osmaniye. These quakes are the biggest to have struck Turkey in the last century and the most important to have occurred in the south-east of the nation in hundreds of years.

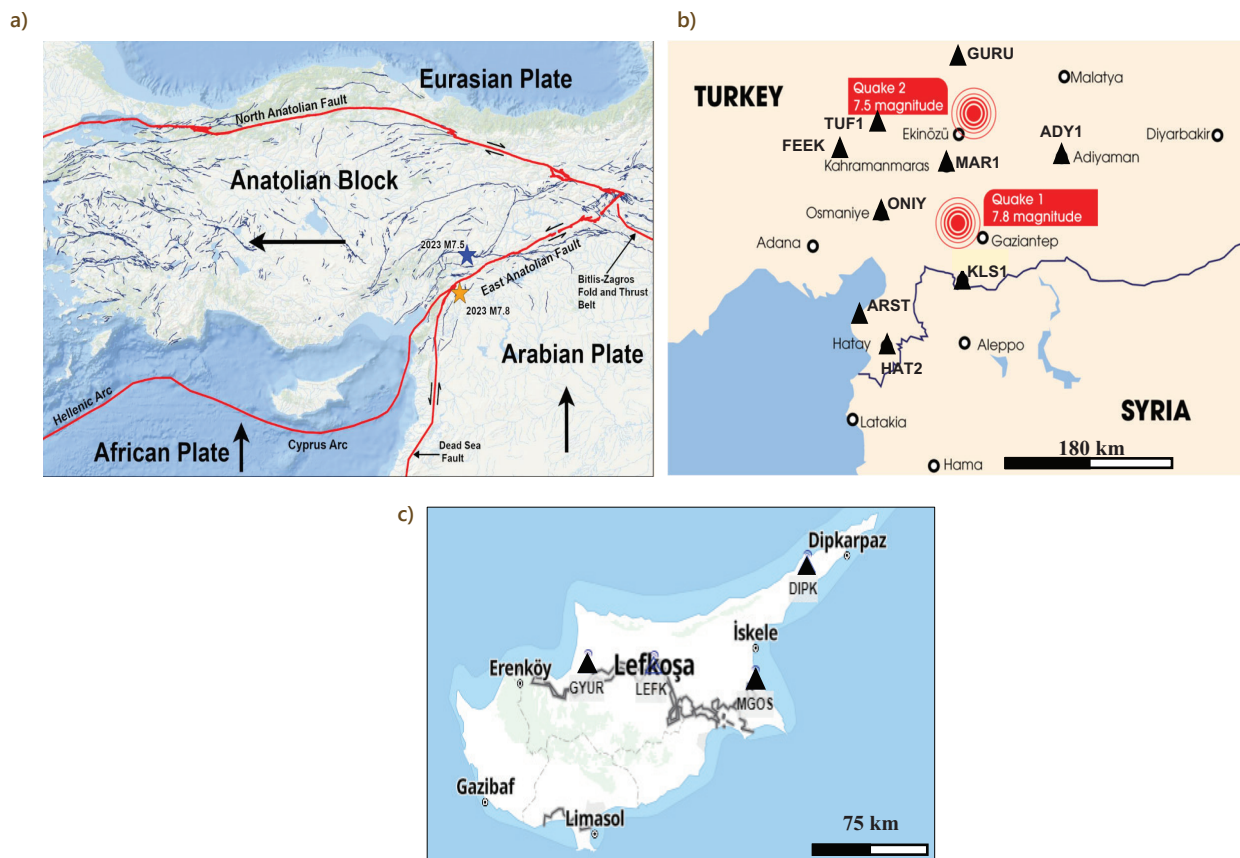


Figure 1. Kahramanmaraş earthquake series and Cyprus Arc, Dead Sea fault: a – Anatolian Block, African, Arabian, Eurasian Plate and the epicenters of two Kahramanmaraş earthquakes; b – this was the case the morning of February 6, 2023, as a 7.8 magnitude earthquake shook parts of Turkey and Syria. Nine hours later, a 7.5 magnitude earthquake struck and (b) and (c) CORS-TR stations in the study region

3. Results

3.1. GNSS surveys (two earthquakes, 06.02.2023)

It is vital to realize the tectonic mechanics involved in order to fully appreciate the magnitudes of the displacements caused by the Kahramanmaraş earthquakes in Pazarcik and Elbistan. In this situation, data from CORS-TR stations close to the earthquake epicenter is quite helpful. Data from this network's CORS-TR stations are kept at 1-second intervals and are particularly suitable in identifying earthquakes and crustal deformations. In this study, data from CORS-TR stations on the CORS-TR network close to the epicenter of the Kahramanmaraş (06.02.2023) earthquakes was examined and evaluated (Figures 1 and 2). As shown in Figures 2, 3, 4, 5, 6, 7, 8, 9, 10, 11, 12 and 13, the earthquake displacements were computed by examining the time series produced from the daily solutions (February 6, 2023).

The CORS-TR stations' coordinates and standard deviations on February 5, 2023, as determined by the static method, are shown in Table 1. On February 5, 2023, the horizontal and vertical coordinate standard deviations were computed with an accuracy of 2–3 mm and 8–14 mm, respectively (Table 1). To explore the earthquake effects visible in the time series, the data from February 6th, 2023 were processed (kinematic-static method) (00:00:00–11:15:00 UTC time). At this time RINEX observation data with 1-second intervals were downloaded from the CORS-TR servers. The RINEX observation data (06.02.2023) of CORS-TR stations were investigated by using the CSRS-PPP Software to process both static (1 sec interval) and kinematic (00:00:00–11:15:00 UTC time, 1 sec interval) methods. Results from static and kinematic processing were gained by using the CSRS-PPP Software. The coordinates derived from using the static method were compared with the coordinates by utilizing the kinematic method. Figures 2, 3, 4,

5, 6, 7, 8, 9, 10, 11, 12 and 13 depict how these CORS-TR stations were affected by the Kahramanmaraş-centered earthquakes.

3.2. Stations near two earthquakes (06.02.2023)

Since the epicenters of the two major earthquakes that occurred on February 6, 2023 are very close to Kahramanmaraş, GNSS satellite data of MAR1 station could not be obtained during the first and second earthquakes. Instead of these data, GNSS satellite observations of February 5, 2023 and February 10, 2023 were processed and the three dimensional displacements caused by the two earthquakes of MAR1 station were obtained. Horizontal and vertical displacements are computed about 61.55 cm and –4.7 cm (collapse), respectively. The motion caused by two earthquakes at the MAR1 station was obtained in the south-west direction, see Figure 2.

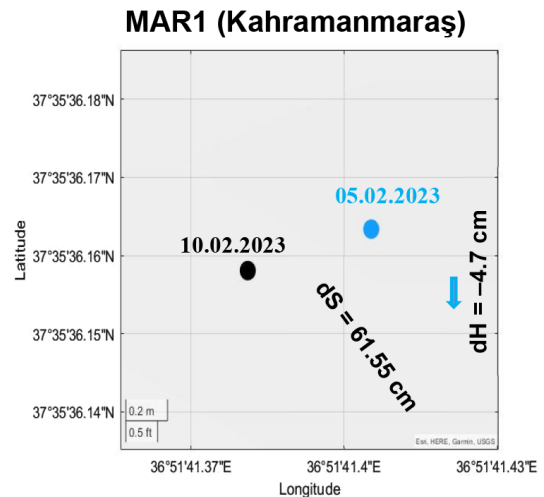


Figure 2. The horizontal and vertical displacement values of MAR1 (Kahramanmaraş) station between February 5, 2023 and February 10, 2023

Table 1. Standard deviations and ITRF20 (2023.1 Epoch) coordinates of CORS-TR stations near the region of the Kahramanmaraş earthquakes on 05.02.2023

Station	φ_{ITRF}	λ_{ITRF}	h_{ITRF} (m)	Std (X) [mm]	Std (Y) [mm]	Std (h) [mm]
MAR1	37°35'36.16338"	36°51'41.40531"	734,468	2	2	8
HAT2	36°11'44.01917"	36°8'41.74593"	137,367	2	2	8
ADY1	37°45'38.10067"	38°15'40.47353"	741,173	2	2	8
FEEK	37°48'54.42663"	35°54'44.38430"	600,289	2	2	8
DIPK	35°32'12.84021"	34°11'40.80393"	155,289	2	2	8
GURU	38°43'2.47881"	37°18'28.33543"	1357,452	3	2	8
GYUR	35°12'04.50191"	32°59'21.10010"	78,951	2	2	8
KLS1	36°42'45.32660"	37°7'25.20143"	660,821	2	2	8
MGOS	35°8'44.96520"	33°54'26.60914"	49,778	2	2	8
ONİY	37°6'7.90567"	36°15'13.89945"	127,196	2	2	8
TUF1	38°15'37.97170"	36°12'30.41617"	1504,775	2	2	8
ARST	36°24'56.13140"	35°53'6.53228"	31,122	2	2	8

GNSS satellite data could only be recorded for a short time after the end of the first earthquake at ADY1 point, Figure 3a. For this reason, the coordinates were obtained by processing these GNSS satellite observations of ADY1 on February 5, 2023 and February 20, 2023. As seen in Figure 3d, the horizontal displacement is about 68.97 cm in the south-east direction, while the vertical displacement is -0.75 cm (collapse) at ADY1 station. At the initial time of the first earthquake, the reactive movement of the ADY1 station was obtained as 40 cm in the north-east direction, Figure 3b. In the vertical displacement at ADY1 point, a swelling-collapsing movements of 10–15 cm was totally computed (Figures 3a and 3c).

At ONIY point, GNSS satellite data were recorded in a short time after the first earthquake, Figure 4a. Figure 4d was obtained by processing GNSS satellite data on 5 February 2023 and on 10 February 2023 at ONIY station. As seen in Figure 4d, the horizontal displacement was calculated as 33.23 cm in the south-west direction, while the

vertical displacement was calculated about 5 cm (collapse) at ONIY station. At the initial time of the first earthquake, the reactive movement of the ONIY point was obtained as 34 cm in the south-west direction. In the vertical position at ONIY point, a collapsing movement about 5 cm was observed (Figures 4a and 4c).

Horizontal and vertical coordinate differences of FEEK station are shown in Figure 5a. In Figure 5b, the position of the FEEK station during the first earthquake and the second earthquake and its instantaneous vector movements are shown. In Figure 5c, the position and vector movements of two earthquakes are shown in three dimensions. Figure 5d shows the location of the FEEK point on February 5, 2023 (blue circle), the position at the first earthquake on February 6, 2023 (red circle), and the position at the second earthquake on February 6, 2023 (black circle). As seen in Figure 5d at the FEEK point, the horizontal displacement obtained after the first earthquake was 8.93 cm in the south-west direction, while this movement

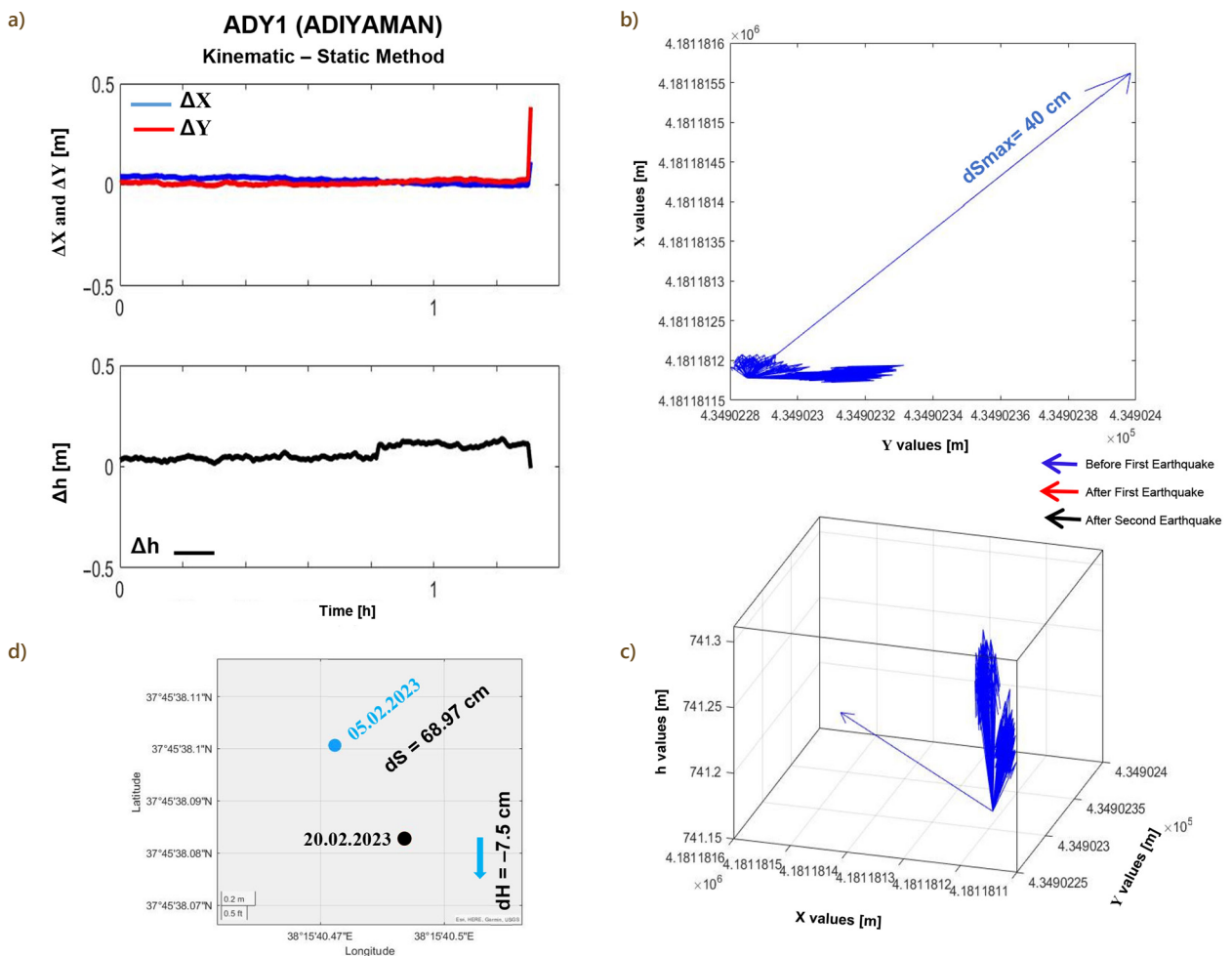


Figure 3. Horizontal and vertical motion of ADY1 (Adiyaman) station: a – a time series of the horizontal and vertical coordinate discrepancies obtained at 30-second intervals from the ADY1 CORS-TR station during the first Kahramanmaraş earthquakes (04:17:35); b – the ADY1 CORS-TR station’s horizontal displacement vectors for the February 6, 2023, first, second, and pre-earthquakes (00:00:00–01:19:30 UTC time); c – 3D displacement vectors attributable to the earthquake that occurred on February 6, 2023 at ADY1 CORS-TR station; d – horizontal and vertical displacements of ADY1 station after first earthquake

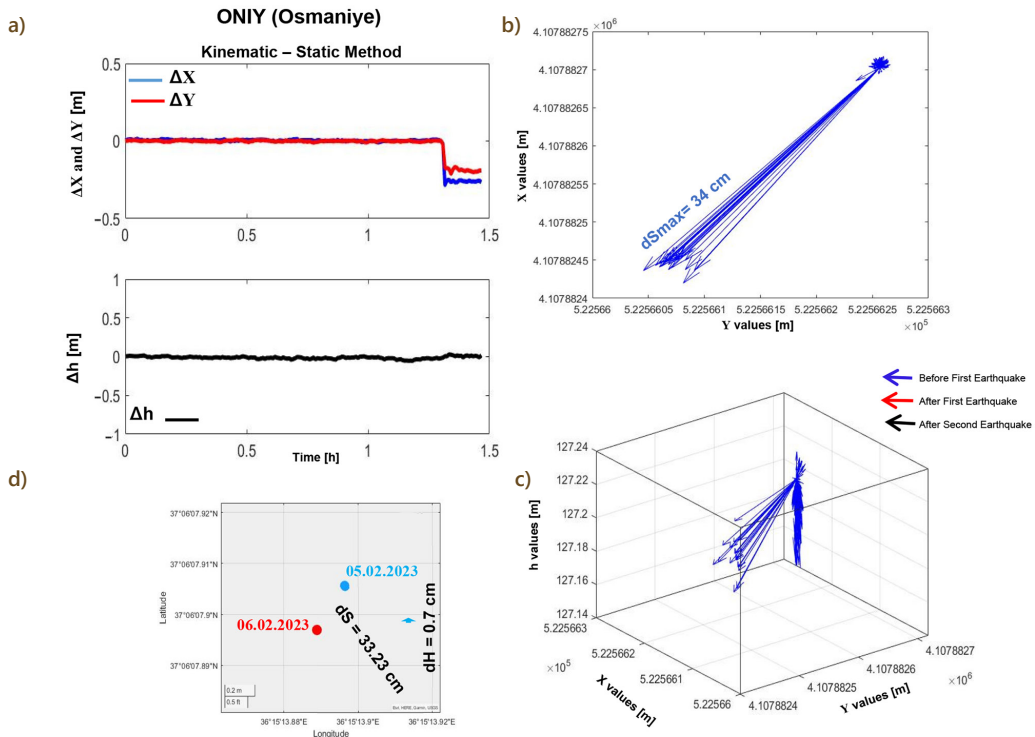


Figure 4. Horizontal and vertical motion of ONIY (Osmaniye) station: a – a time series of the horizontal and vertical coordinate discrepancies obtained at 30-second intervals from the ONIY (Osmaniye) CORS-TR station between the two Kahramanmaraş earthquakes (04:17:35 and 13:24:49 Local time); b – the ONIY CORS-TR station's horizontal displacement vectors for the February 6, 2023, first, second, and pre-earthquakes (00:00:00–01:30:00 UTC time); c – 3D displacement vectors attributable to the earthquake that occurred on February 6, 2023 at ONIY CORS-TR station; d – horizontal and vertical displacements of ONIY station after first earthquake

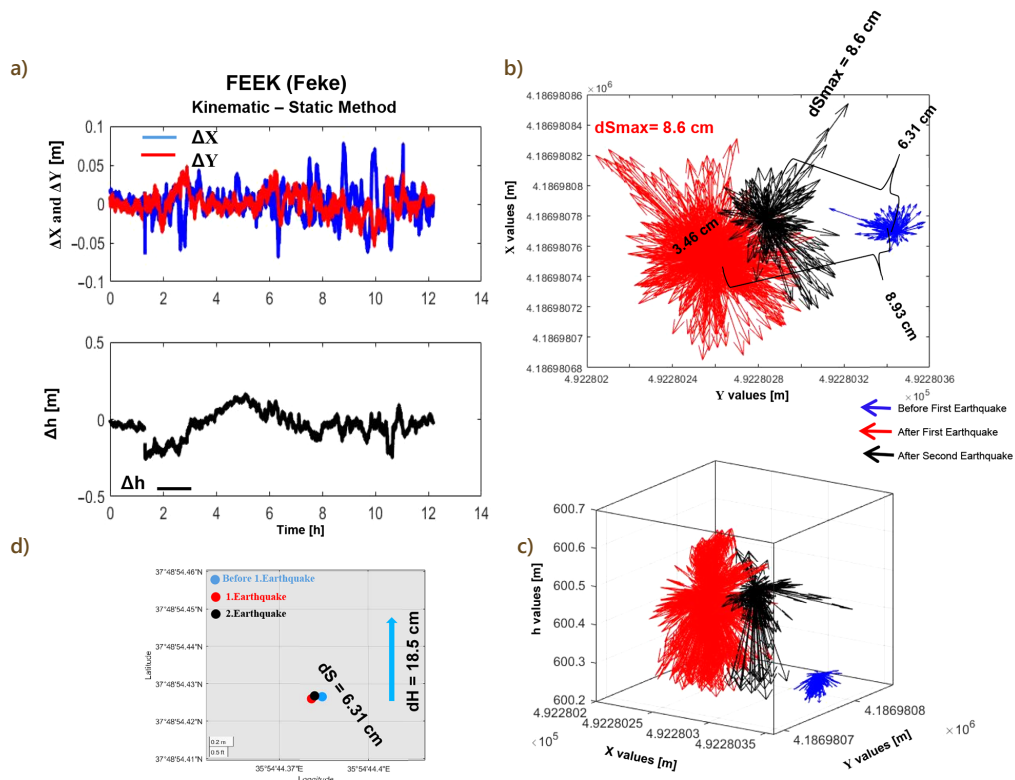


Figure 5. Horizontal and vertical motion of FEEK (Feke) station: a – a time series of the horizontal and vertical coordinate discrepancies obtained at 30-second intervals from the FEEK (Feke) CORS-TR station between the two Kahramanmaraş earthquakes (04:17:35 and 13:24:49 Local time); b – the FEEK CORS-TR station's horizontal displacement vectors for the February 6, 2023, first, second, and pre-earthquakes (00:00:00–11:59:30 UTC time); c – 3D displacement vectors attributable to the earthquake that occurred on February 6, 2023 at FEEK CORS-TR station; d – horizontal and vertical displacements of FEEK station after two earthquakes

was obtained as 3.46 cm in the north-east direction in the second earthquake. The total displacement value of the horizontal direction was computed as 6.31 cm in the west direction. In the height values, swelling and collapse movements were observed around 18.5 cm at FEEK station, respectively. Thus, the total vertical displacement was approximately 15 cm, Figures 5a and 5c. The instantaneous response movement of FEEK station at the initial time of the first earthquake was calculated as 8.6 cm in the north-west direction, Figure 5b. The instantaneous response movement of FEEK station at the initial time of the second earthquake was calculated as 8.6 cm in the north-east direction, Figure 5b.

Horizontal and vertical coordinate differences of GURU station are shown in Figure 6a. In Figure 6b, the positions of the GURU station during the first earthquake and the second earthquake, and its instantaneous vector movements are shown. In Figure 6c, the position and vector movements of two earthquakes are shown in three dimensions. Figure 6d shows the location of the GURU point on February 5, 2023 (blue circle), the position at the first earthquake on February 6, 2023 (red circle), and the position at the second earthquake on February 6, 2023 (black circle). As seen in Figure 6d at the GURU point, the horizontal displacement obtained after the first earthquake

was 9.23 cm in the south-east direction, while this movement was obtained as 9.57 cm in the north-west direction in the second earthquake. The total displacement value of the horizontal direction was computed as 3.80 cm in the south direction. In the height values, swelling and collapse movements were observed around 15–20 cm at GURU station, respectively. Thus, the total vertical displacement was approximately 50 cm, Figures 6a and 6c. The instantaneous response movement of GURU station at the initial time of the first earthquake was calculated as 7.7 cm in the north direction, Figure 6b. The instantaneous response movement of GURU station at the initial time of the second earthquake was calculated as 23.3 cm in the east direction, Figure 6b.

GNSS data of the period of the first earthquake at KLS1 station could not be obtained, see Figure 7. Horizontal and vertical coordinate differences of KLS1 station are shown in Figure 7a. In Figure 7b, the positions of the KLS1 station during the first earthquake and the second earthquake, and its instantaneous vector movements are shown. In Figure 7c, the position and vector movements of two earthquakes are shown in three dimensions. Figure 7d shows the location of the KLS1 point on February 5, 2023 (blue circle), the position at the first earthquake on February 6, 2023 (red circle), and the position at the second earthquake on February 6, 2023 (black circle). As seen in

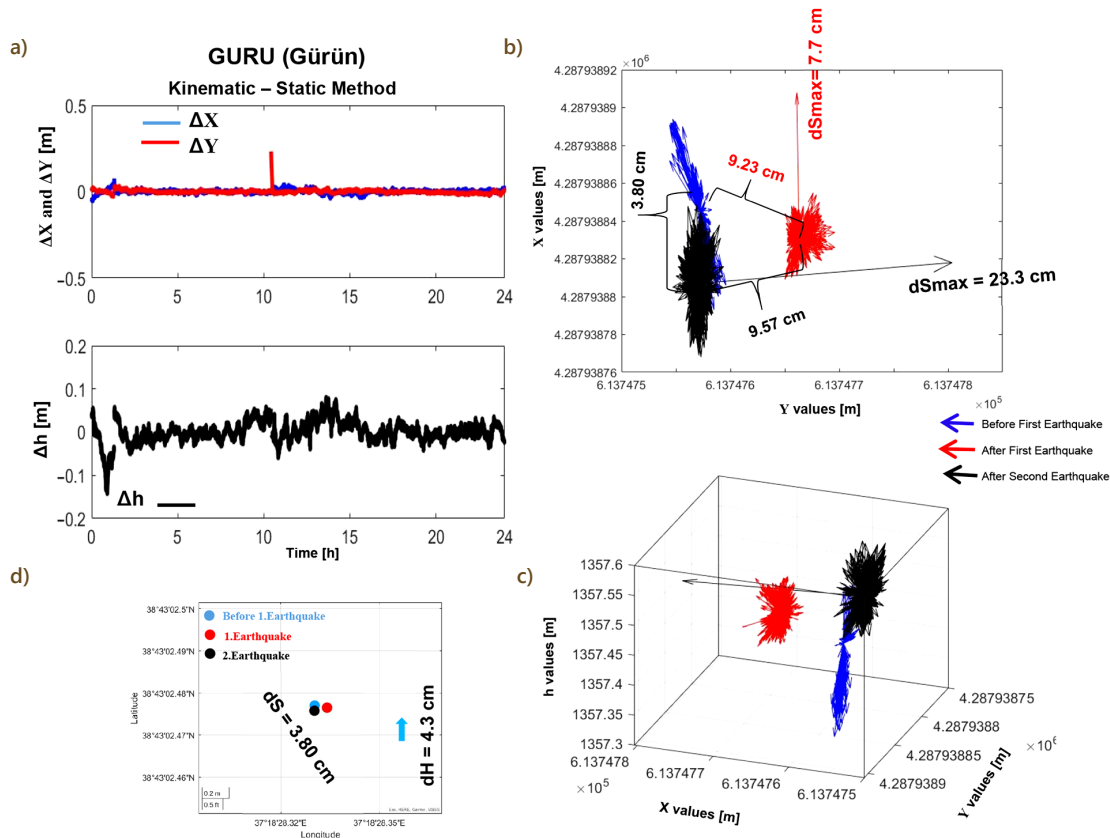


Figure 6. Horizontal and vertical motion of GURU (Gürün) station: a – a time series of the horizontal and vertical coordinate discrepancies obtained at 30-second intervals from the GURU (Gürün) CORS-TR station between the two Kahramanmaraş earthquakes (04:17:35 and 13:24:49 Local time); b – the GURU CORS-TR station’s horizontal displacement vectors for the February 6, 2023, first, second, and pre-earthquakes (00:00:00–23:59:30 UTC time); c – 3D displacement vectors attributable to the earthquake that occurred on February 6, 2023 at GURU CORS-TR station; d – horizontal and vertical displacements of GURU station after two earthquakes

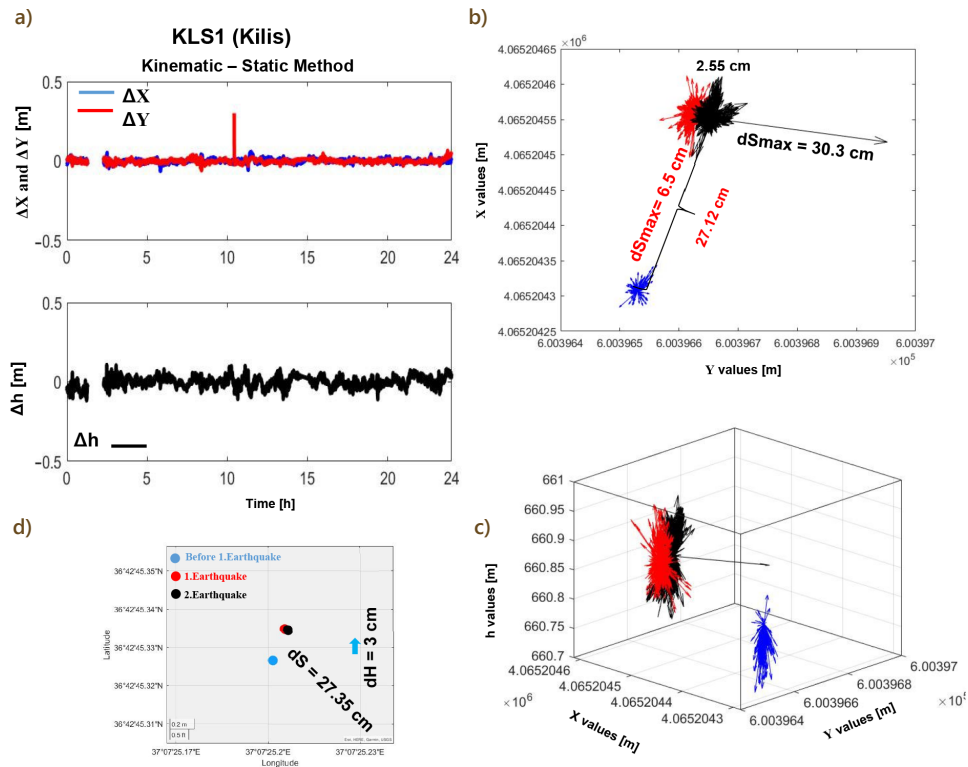


Figure 7. Horizontal and vertical motion of KLS1 (Kilis) station: a – a time series of the horizontal and vertical coordinate discrepancies obtained at 30-second intervals from the KLS1 (Kilis) CORS-TR station between the two Kahramanmaraş earthquakes (04:17:35 and 13:24:49 Local time); b – the KLS1 CORS-TR station's horizontal displacement vectors for the February 6, 2023, first, second, and pre-earthquakes (00:00:00–23:59:30 UTC time); c – 3D displacement vectors attributable to the earthquake that occurred on February 6, 2023 at KLS1 CORS-TR station; d – horizontal and vertical displacements of KLS1 station after two earthquakes

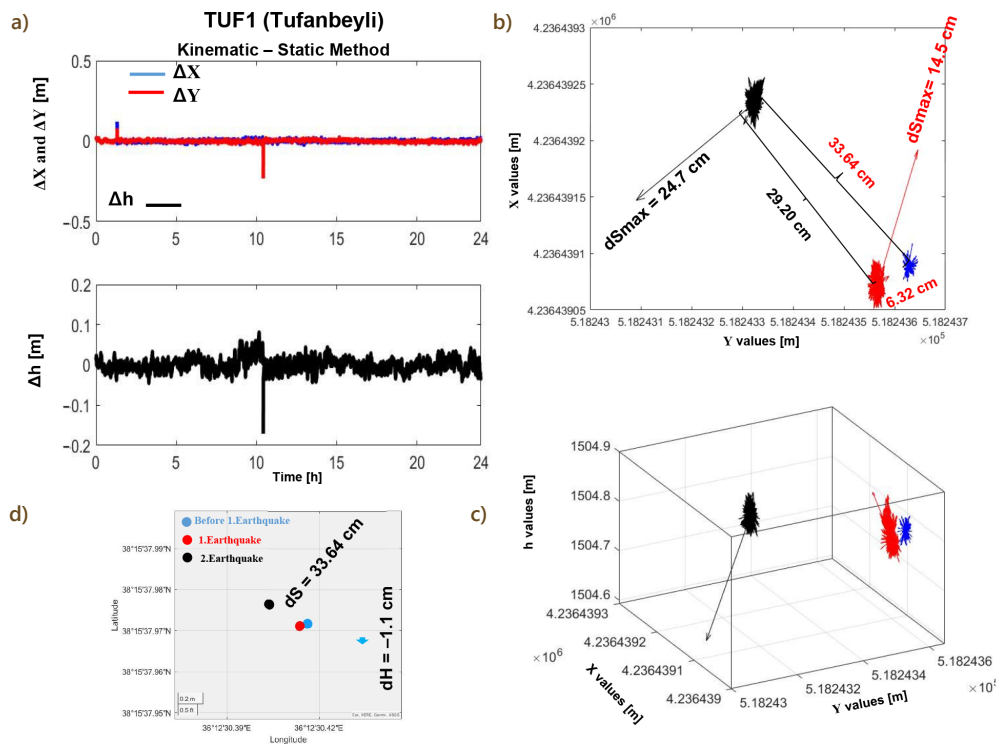


Figure 8. Horizontal and vertical motion of TUF1 (Tufanbeyli) station: a – a time series of the horizontal and vertical coordinate discrepancies obtained at 30-second intervals from the TUF1 CORS-TR station between the two Kahramanmaraş earthquakes (04:17:35 and 13:24:49 Local time); b – the TUF1 CORS-TR station's horizontal displacement vectors for the February 6, 2023, first, second, and pre-earthquakes (00:00:00–23:59:30 UTC time); c – 3D displacement vectors attributable to the earthquake that occurred on February 6, 2023 at TUF1 CORS-TR station (00:00:00–11:15:00 UTC time)

Figure 7d at the KLS1 point, the horizontal displacement obtained after the first earthquake was 27.12 cm in the north-west direction, while this movement was obtained as 2.55 cm in the south-east direction in the second earthquake. The total displacement value of the horizontal direction was computed as 27.35 cm in the north-west direction. In the height values, swelling and collapse movements were observed around 15–20 cm at KLS1 station, respectively.

Thus, the total vertical displacement was approximately 10 cm, Figures 7a and 7c. The instantaneous response movement of KLS1 station at the initial time of the first earthquake was calculated as 6.5 cm in the south direction, Figure 7b. The instantaneous response movement of KLS1 station at the initial time of the second earthquake was calculated as 30.3 cm in the east direction, Figure 7b.

Horizontal and vertical coordinate differences of TUF1 station are shown in Figure 8a. In Figure 8b, the positions of the TUF1 station during the first earthquake and the second earthquake, and its instantaneous vector movements are shown. In Figure 8c, the position and vector

movements of two earthquakes are shown in three dimensions. Figure 8d shows the location of the TUF1 point on February 5, 2023 (blue circle), the position at the first earthquake on February 6, 2023 (red circle), and the position at the second earthquake on February 6, 2023 (black circle). As seen in Figure 8d at the TUF1 point, the horizontal displacement obtained after the first earthquake was 6.32 cm in the south-west direction, while this movement was obtained as 29.20 cm in the north-east direction in the second earthquake. The total displacement value of the horizontal direction was computed as 33.64 cm in the south direction. In the height values, swelling and collapse movements were observed around 15–20 cm at TUF1 station, respectively. Thus, the total vertical displacement was approximately 20 cm, Figures 8a and 8c. The instantaneous response movement of TUF1 station at the initial time of the first earthquake was calculated as 14.5 cm in the north-east direction, Figure 8b. The instantaneous response movement of TUF1 station at the initial time of the second earthquake was calculated as 24.7 cm in the south-west direction, Figure 8b.

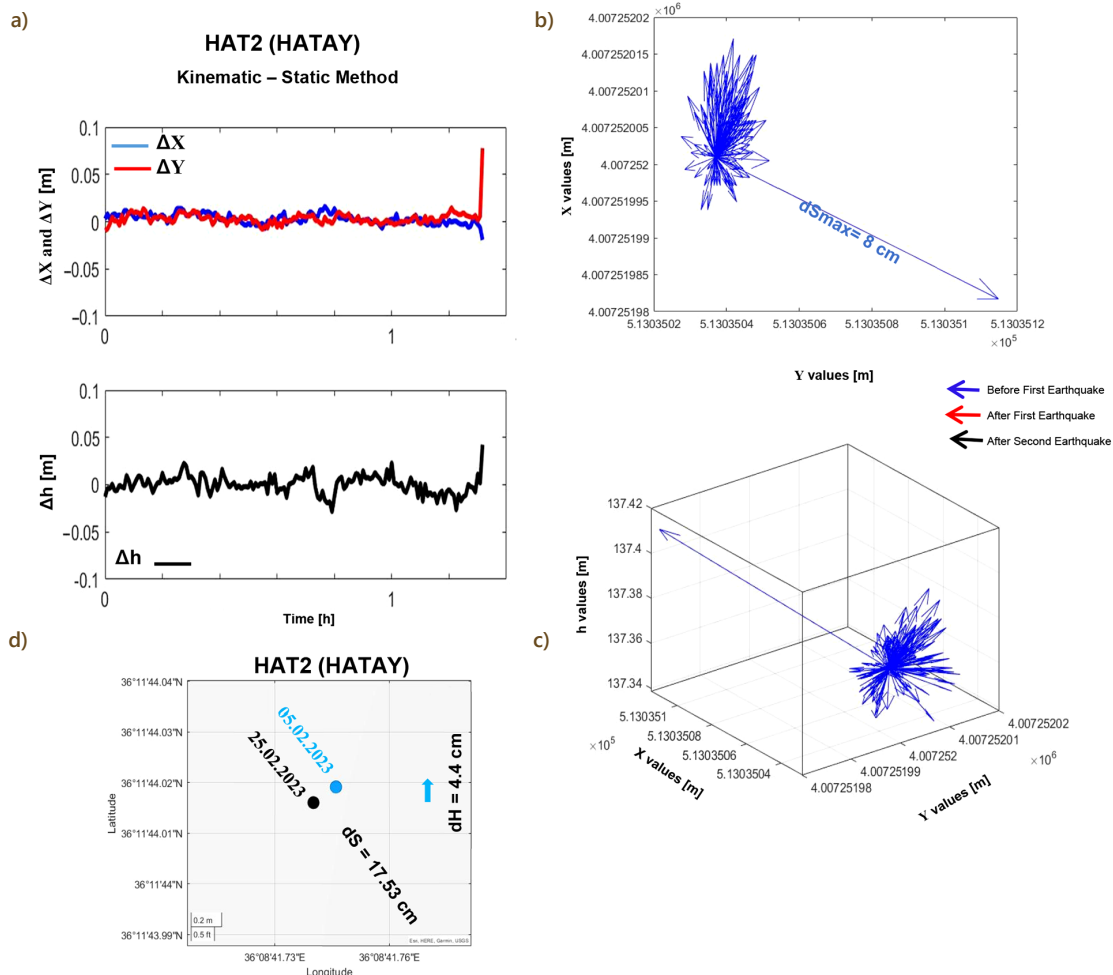


Figure 9. Horizontal and vertical motion of HAT2 (Hatay) station: a – a time series of the horizontal and vertical coordinate discrepancies obtained at 30-second intervals from the HAT2 (Hatay) CORS-TR station during the first Kahramanmaraş earthquake (04:17:35 Local time); b – The HAT2 CORS-TR station’s horizontal displacement vectors for the February 6, 2023, first, second, and pre-earthquakes (00:00:00–01:24:00 UTC time); c – 3D displacement vectors attributable to the earthquake that occurred on February 6, 2023 at HAT2 CORS-TR station; d – horizontal and vertical displacements of HAT2 station after two earthquakes

3.3. Hatay region

At HAT2 station, just as in ADY1 point, GNSS satellite data were recorded in a short time after the first earthquake, see Figure 9. Figure 9d was obtained by processing GNSS satellite data on 5 February 2023 and the satellite data on 25 February 2023 at HAT2 point. As seen in Figure 9d, the horizontal displacement was calculated as 17.53 cm in the south-west direction, while the vertical displacement was calculated as 4.4 cm (swell). At the initial time of the first earthquake, the reactive movement of the HAT2 point was obtained as 8 cm in the south-east direction. In the vertical position at HAT2 point, a swelling movement of about 5 cm was observed (Figure 9c).

Horizontal and vertical coordinate differences of ARST station are shown in Figure 10a. In Figure 10b, the position of the ARST station during the first earthquake and the second earthquake, and its instantaneous vector movements are shown. In Figure 10c, the position and vector movements of two earthquakes are shown in three dimensions. Figure 10d shows the location of the ARST point on February 5, 2023 (blue circle), the position at the first earthquake on February 6, 2023 (red circle), and the position at the second earthquake on February 6, 2023 (black circle). As seen in Figure 10d at the ARST point, the

horizontal displacement obtained after the first earthquake was 29.78 cm in the west direction, while this movement was obtained as 1.33 cm in the north-east direction in the second earthquake. The total displacement value of the horizontal direction was computed as 28.54 cm in the west direction. In the height values, swelling movements were observed around 5 cm at ARST station. Thus, the total vertical displacement was approximately 5 cm, Figures 10a and 10c. On the other hand, the instantaneous response movement of ARST station at the initial time of the first earthquake was computed as 25.3 cm in the south-east direction, Figure 10b.

3.4. Stations on Cyprus Arc

Horizontal and vertical coordinate differences of DIPK station are shown in Figure 11a. In Figure 11b, the position of the DIPK station during the first earthquake and the second earthquake, and its instantaneous vector movements are shown. In Figure 11c, the position and vector movements of two earthquakes are shown in three dimensions. Figure 11d shows the location of the DIPK point on February 5, 2023 (blue circle), the position at the first earthquake on February 6, 2023 (red circle), and the position at the second earthquake on February 6, 2023 (black

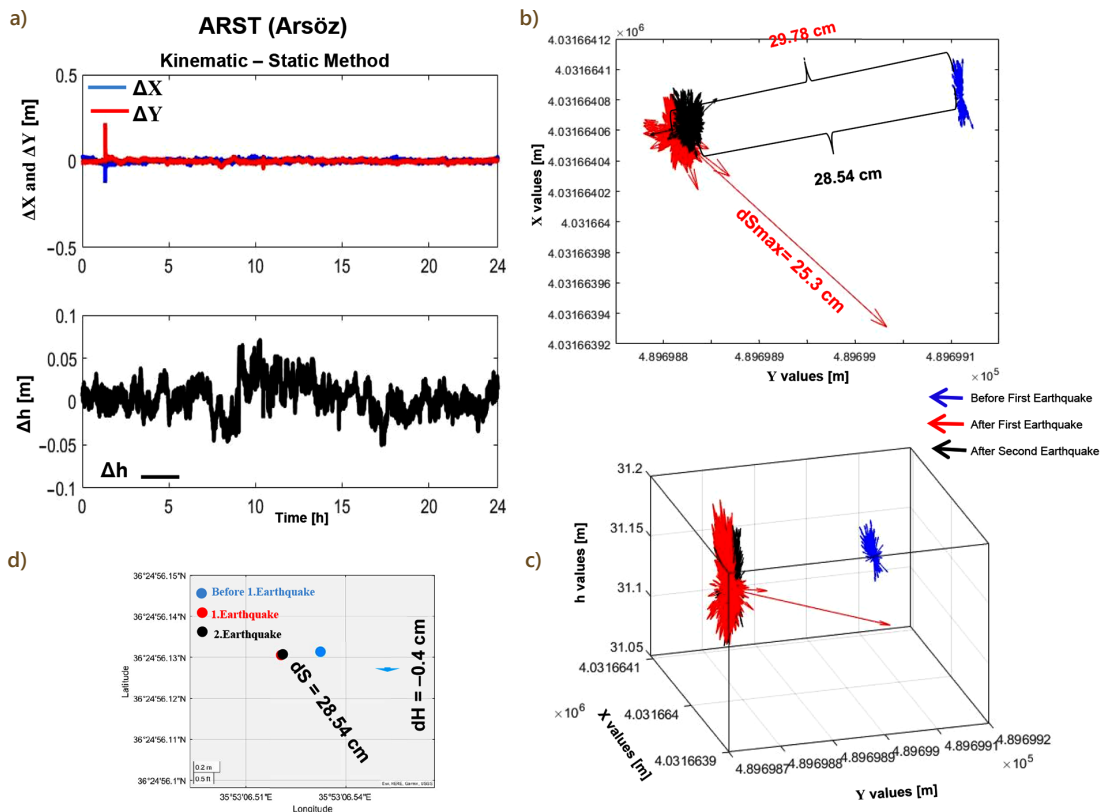


Figure 10. Horizontal and vertical motion of ARST (Arsöz) station: a – a time series of the horizontal and vertical coordinate discrepancies obtained at 30-second intervals from the ARST (Arsöz) CORS-TR station between the two Kahramanmaraş earthquakes (04:17:35 and 13:24:49 Local time); b – the ARST CORS-TR station's horizontal displacement vectors for the February 6, 2023, first, second, and pre-earthquakes (00:00:00–23:59:30 UTC time); c – 3D displacement vectors attributable to the earthquake that occurred on February 6, 2023 at ARST CORS-TR station; d – horizontal and vertical displacements of ARST station after two earthquakes

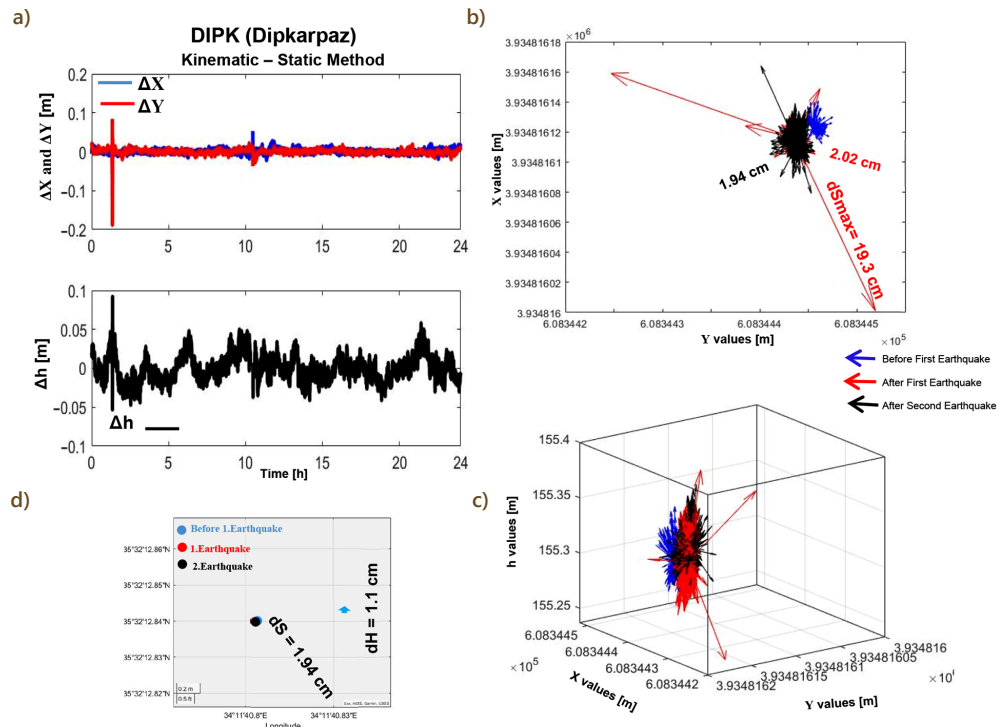


Figure 11. Horizontal and vertical motion of DPK (Dipkarpaz) station: a – a time series of the horizontal and vertical coordinate discrepancies obtained at 30-second intervals from the DPK (Dipkarpaz) CORS-TR station between the two Kahramanmaraş earthquakes (04:17:35 and 13:24:49 Local time); b – the DPK CORS-TR station’s horizontal displacement vectors for the February 6, 2023, first, second, and pre-earthquakes (00:00:00–23:59:30 UTC time); c – 3D displacement vectors attributable to the earthquake that occurred on February 6, 2023 at DPK CORS-TR station; d – horizontal and vertical displacements of DPK station after two earthquakes

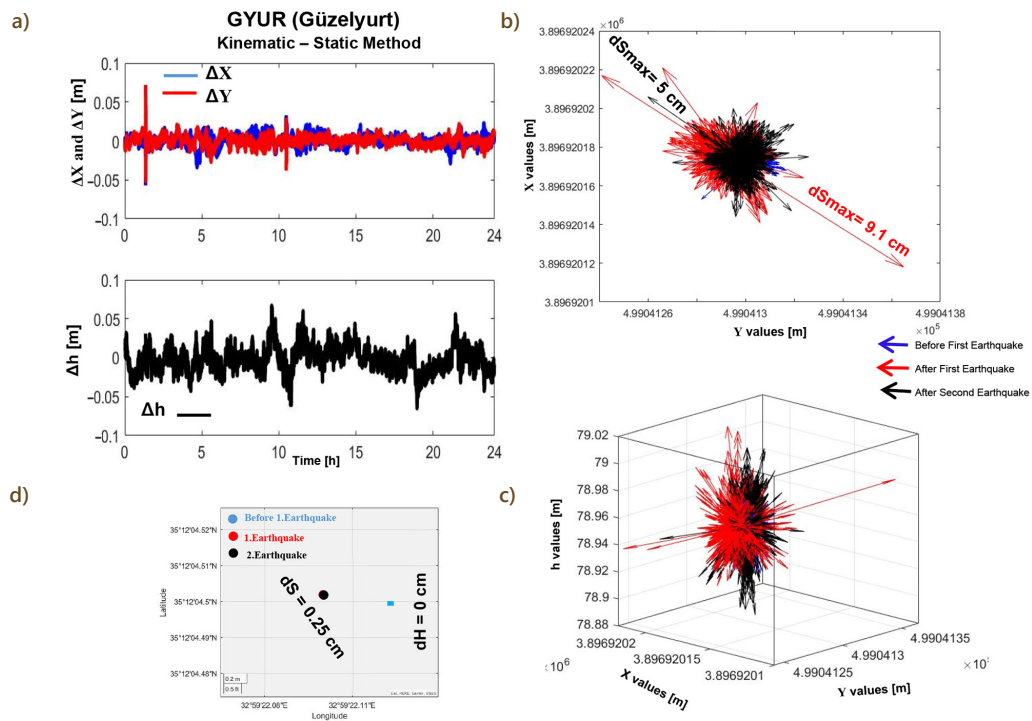


Figure 12. Horizontal and vertical motion of GYUR (Güzelyurt) station: a – a time series of the horizontal and vertical coordinate discrepancies obtained at 30-second intervals from the GYUR (Güzelyurt) CORS-TR station between the two Kahramanmaraş earthquakes (04:17:35 and 13:24:49 Local time); b – the GYUR CORS-TR station’s horizontal displacement vectors for the February 6, 2023, first, second, and pre-earthquakes (00:00:00–23:59:30 UTC time); c – 3D displacement vectors attributable to the earthquake that occurred on February 6, 2023 at GYUR CORS-TR station; d – horizontal and vertical displacements of GYUR station after two earthquakes

circle). As seen in Figure 11d at the DIPK point, the horizontal displacement obtained after the first earthquake was 2.02 cm in the south-west direction, while this movement was obtained as 0.53 cm in the north-east direction in the second earthquake. The total displacement value of the horizontal direction was computed as 1.94 cm in the south-west direction. In the height values, collapse and swelling movements were observed around 5–10 cm at DIPK station, respectively. Thus, the total vertical displacement was approximately 15 cm, Figures 11a and 11c. On the other hand, the instantaneous response movement of DIPK station at the initial time of the first earthquake was calculated as 19.3 cm in the south-east direction, Figure 11b.

Horizontal and vertical coordinate differences of GYUR station are shown in Figure 12a. In Figure 12b, the position of the GYUR station during the first earthquake and the second earthquake, and its instantaneous vector movements are shown. In Figure 12c, the position and vector movements of two earthquakes are shown in three dimensions. Figure 12d shows the location of the GYUR point on February 5, 2023 (blue circle), the position at the first earthquake on February 6, 2023 (red circle), and the position at the second earthquake on February 6, 2023 (black

circle). As seen in Figure 12d at the GYUR point, the horizontal displacement obtained after the first earthquake was 0.76 cm in the south-west direction, while this movement was obtained as 0.65 cm in the north-east direction in the second earthquake. The total displacement value of the horizontal direction was computed as 0.25 cm in the south direction. In the height values, swelling and collapse movements were observed around 5–7 cm at GYUR station, respectively. Thus, the total vertical displacement was approximately 15 cm, Figure 12c. On the other hand, the instantaneous response movement of GYUR station at the initial time of the first earthquake was calculated as 9.1 cm in the south-east direction, Figure 12b. The instantaneous response movement of GYUR station at the initial time of the second earthquake was calculated as 5 cm in the north-west direction, Figure 12b.

Horizontal and vertical coordinate differences of MGOS station are shown in Figure 13a. In Figure 13b, the position of the MGOS station during the first earthquake and the second earthquake, and its instantaneous vector movements are shown. In Figure 13c, the position and vector movements of two earthquakes are shown in three dimensions. Figure 13d shows the location of the MGOS point on February 5, 2023 (blue circle), the position at the first

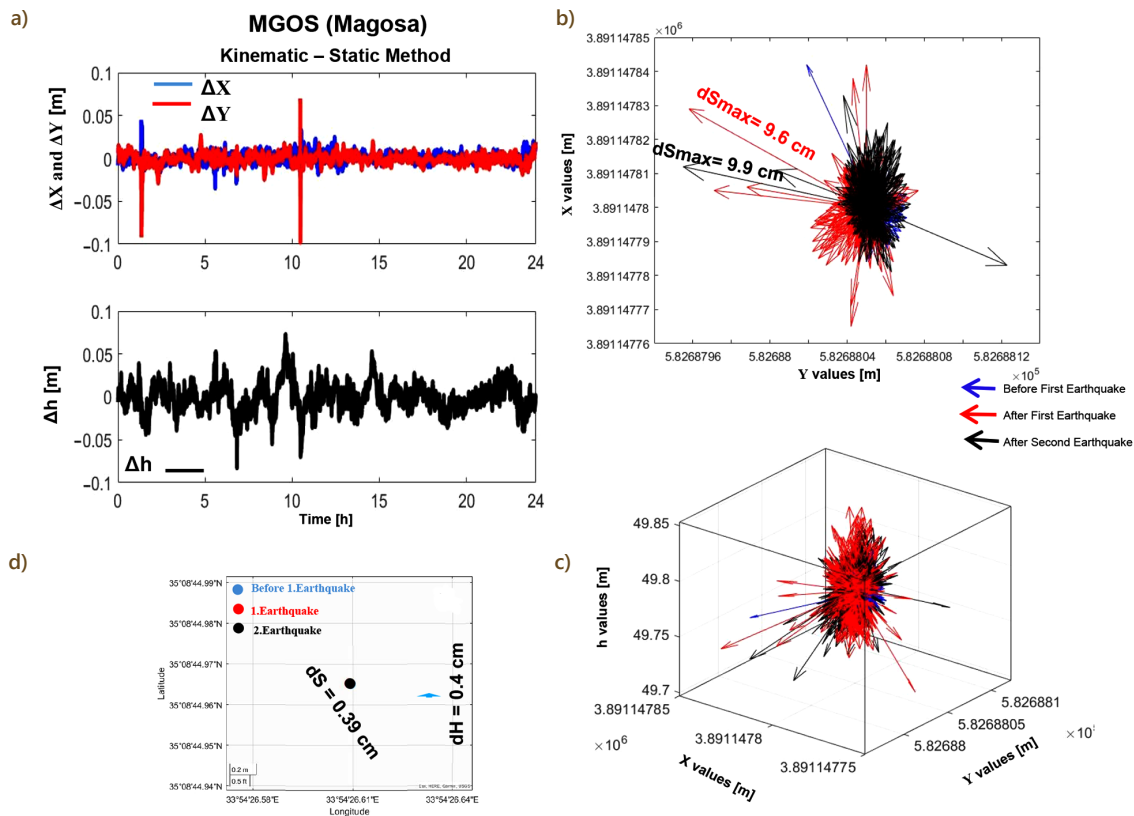


Figure 13. Horizontal and vertical motion of MGOS (Magosa) station: a – a time series of the horizontal and vertical coordinate discrepancies obtained at 30-second intervals from the MGOS (Magosa) CORS-TR station between the two Kahramanmaraş earthquakes (04:17:35 and 13:24:49 Local time); b – the MGOS CORS-TR station's horizontal displacement vectors for the February 6, 2023, first, second, and pre-earthquakes (00:00:00–23:59:30 UTC time); c – 3D displacement vectors attributable to the earthquake that occurred on February 6, 2023 at MGOS CORS-TR station; d – horizontal and vertical displacements of MGOS station after two earthquakes

earthquake on February 6, 2023 (red circle), and the position at the second earthquake on February 6, 2023 (black circle). As seen in Figure 13d at the MGOS point, the horizontal displacement obtained after the first earthquake was 0.68 cm in the south-west direction, while this movement was obtained as 0.31 cm in the north-east direction in the second earthquake. The total displacement value of the horizontal direction was computed as 0.39 cm in the south direction. In the height values, swelling and collapse movements were observed around 15–20 cm at MGOS station, respectively. Thus, the total vertical displacement was approximately 50 cm, Figure 13c. The instantaneous response movement of MGOS station at the initial time of the first earthquake was calculated as 9.6 cm in the north-west direction, Figure 13b. The instantaneous response movement of MGOS station at the initial time of the second earthquake was calculated as 9.9 cm in the west direction, Figure 13b.

At the selected points close to the center of the two earthquakes, the instantaneous splash movements of the two earthquakes are in the south-west direction (at MAR1, ONIY, KLS1, TUF1 stations), in the north-east direction (at ADY1, FEKE, TUF1 stations), in the north-west direction (at FEKE station) in the north and east directions (at GURU station) and south direction (at KLS1 station) was obtained. This movement was obtained in the south-east direction (at HAT2, ARST stations) in the Hatay region. For the Cyprus Arc, this movement was obtained in the south-east, north-west and west directions (at DIPK, GYUR and MGOS stations).

4. Conclusions

The accurate coordinates of the network stations near the epicenters of the Kahramanmaraş earthquakes in Turkey were examined by using the precise point positioning (PPP) approach, which is described in this study. The CSRS-PPP service then assesses the network baseline horizontal displacements in the three directions of X, Y, and H. It was clear that the PPP approach produces correct results for point displacement. It is crucial to utilize a processing tool that produces correct results in order to assure the displacements and results for each point since any mistake while submitting raw data of points or an error in the user datum results in a big inaccuracy in the results. In the obtained results, it was computed that the greatest horizontal displacement occurred at the HAT2 station with 68.97 cm in two earthquakes. At the selected points close to the center of the two earthquakes, the instantaneous splash movements of the two earthquakes are in the south-west direction (at MAR1, ONIY, KLS1, TUF1 stations), in the north-east direction (at ADY1, FEKE, TUF1 stations), in the north-west direction (at FEKE station) in the north and east directions (at GURU station) and south direction (at KLS1 station) was obtained. This movement was obtained in the south-east direction (at HAT2, ARST stations) in the Hatay region. For the Cyprus arc, this movement was

obtained in the south-east, north-west and west directions (for DIPK, GYUR and MGOS stations).

References

- Aktug, B., Ozener, H., Dogru, A., Sabuncu, A., Turgut, B., Halicioglu, K., Yilmaz, O., & Havazli, E. (2016). Slip rates and seismic potential on the East Anatolian Fault System using an improved GPS velocity field. *Journal of Geodynamics*, 94–95, 1–12. <https://doi.org/10.1016/j.jog.2016.01.001>
- Akyuz, H. S., Altunel, E., Karabacak, V., & Yalciner, C. C. (2006). Historical earthquake activity of the northern part of the Dead Sea Fault Zone, southern Turkey. *Tectonophysics*, 426(3–4), 281–293. <https://doi.org/10.1016/j.tecto.2006.08.005>
- Ambraseys, N. N. (2009). *Earthquakes in the Eastern Mediterranean and the Middle East: A multidisciplinary study of 2000 years of seismicity*. Cambridge University Press. <https://doi.org/10.1017/CBO9781139195430>
- CSRS-PPP Online Processing. (2023). <https://webapp.csrscs-crscnrcan-rncan.gc.ca/geod/tools-outils/ppp.php>
- Duman, T. Y., & Emre, Ö. (2013). The East Anatolian Fault: Geometry, segmentation and jog characteristics. *Geological Society, London, Special Publications*, 372(1), 495–529. <https://doi.org/10.1144/SP372.14>
- Ehiorobo, J., & Ehigiator Irughe, R. (2012). Evaluation of absolute displacement of geodetic control for dam deformation monitoring using CSRS-PPP model. *Journal of Earth Science and Engineering*, 2, 277–286.
- Elhadidy, M., Abdalzaheer, M. S., & Gaber, H. (2021). Up-to-date PSHA along the Gulf of Aqaba-Dead Sea transform fault. *Soil Dynamics and Earthquake Engineering*, 148, Article 106835. <https://doi.org/10.1016/j.soildyn.2021.106835>
- Emre, Ö., Duman, T. Y., Özalp, S., Saroğlu, F., Olgun, Ş., Elmaci, H., & Çan, T. (2018). Active fault database of Turkey. *Bulletin of Earthquake Engineering*, 16, 3229–3275. <https://doi.org/10.1007/s10518-016-0041-2>
- Hancılar, U., Şeşetyan, K., Çaktı, E., Şafak, E., Yenihayat, N., Malcıoğlu, F. S., Dönmez, K., Tetik, T., & Hakan Süleyman, H. (2023). *Kahramanmaraş – Gaziantep Türkiye M7.7 Earthquake, 6 February 2023* (Strong ground motion and building damage estimations, preliminary report). https://eqe.bogazici.edu.tr/sites/eqe.boun.edu.tr/files/kahramanmaraş-gaziantep_earthquake_06-02-2023_04.17-bogazici_university_earthquake_engineering_department_v6.pdf
- Hofmann-Wellenhof, B., Lichtenegger, H., & Collins, J. (2001). *GPS: Theory and practice* (5th rev. ed.). Springer.
- Mahmoud, Y., Masson, F., Meghraoui, M., Cakir, Z., Alchalbi, A., Yavasoglu, H., Yönlü, O., Daoud, M., Ergintav, S., & Inan, S. (2013). Kinematic study at the junction of the East Anatolian fault and the Dead Sea fault from GPS measurements. *Journal of Geodynamics*, 67, 30–39. <https://doi.org/10.1016/j.jog.2012.05.006>
- Palutoğlu, M., & Sasmaz, A. (2017). 29 November 1795 Kahramanmaraş earthquake, southern Turkey. *Bulletin of the Mineral Research and Exploration*, 155, 187–202. <https://doi.org/10.19111/bulletinofmre.314211>
- Pırtı, A., Hoşbaş, R. G., & Yücel, M. A. (2023). Examination of the Earthquake (Samos Island) in Izmir (30.10.2020) by using CORS-TR GNSS observations and InSAR Data. *KSCE Journal of Civil Engineering*, 27, 135–144. <https://doi.org/10.1007/s12205-022-0392-y>
- Reitman, N. G., Briggs, R. W., Barnhart, W. D., Thompson Jobe, J. A., DuRoss, C. B., Hatem, A. E., Gold, R. D., & Mejstrik, J. D. (2023).

Fault rupture mapping of the 6 February 2023 Kahramanmaraş, Türkiye, earthquake sequence from satellite data (ver. 1.1, February 2024). U.S. Geological Survey data release.

<https://doi.org/10.5066/P98517U2>

Tu, R. (2014). Fast determination of displacement by PPP velocity estimation. *Geophysical Journal International*, 196(3), 1397–1401. <https://doi.org/10.1093/gji/ggt480>

Tarı, U., Tüysüz, O., Genç, Ş. C., Imren, C., Blackwell, B. A. B., Lom, N., Tekeşin, Ö., Üsküplü, S., Altiok, S., & Beyhan, M. (2014). The geology and morphology of the Antakya Graben between the Amik Triple Junction and the Cyprus Arc. *Geodinamica Acta*, 26(1–2), 27–55.

<https://doi.org/10.1080/09853111.2013.858962>

U.S. Geological Survey. (2023). *USGS earthquake catalog*. <https://earthquake.usgs.gov/earthquakes/search/>

Wolf, P. R., & Ghilani, C. D. (2002). *Elementary surveying: An introduction to geomatics* (10th ed.). Prentice Hall Upper Saddle River.